

38

**Rapid #: -1613915****Ariel IP: 128.112.205.74**

Status	Rapid Code	Branch Name	Start Date
Pending	TXA	Main Library	2/15/2008 11:19:49 AM

**CALL #:** TL501 .A3287  
**LOCATION:** TXA :: Main Library :: stk  
**TYPE:** Article CC:CCL  
**JOURNAL TITLE:** Aeronautical Quarterly  
**USER JOURNAL TITLE:** AERONAUTICAL QUARTERLY  
**TXA CATALOG TITLE:** The Aeronautical quarterly.  
**ARTICLE TITLE:** TRIANGULAR EQUILIBRIUM ELEMENT IN SOLUTION OF PLATE BENDING PROBLEMS  
**ARTICLE AUTHOR:** MORLEY LSD  
**VOLUME:** 19  
**ISSUE:** Part 2  
**MONTH:**  
**YEAR:** 1968  
**PAGES:** 149  
**ISSN:** 0001-9259  
**OCLC #:** 1461321  
**CROSS REFERENCE ID:** 383015  
**VERIFIED:**

**BORROWER:** PUL :: Interlibrary Services, Firestone  
**PATRON:** Collaborator, PPPL

**PATRON ID:** -  
**PATRON ADDRESS:** -  
**PATRON PHONE:** -  
**PATRON FAX:** -  
**PATRON E-MAIL:** -  
**PATRON DEPT:** -  
**PATRON STATUS:** -  
**PATRON NOTES:** -



This material may be protected by copyright law (Title 17 U.S. Code)  
System Date/Time: 2/15/2008 1:36:32 PM MST

# The Triangular Equilibrium Element in the Solution of Plate Bending Problems

L. S. D. MORLEY

(Royal Aircraft Establishment, Farnborough)

**Summary:** Further details are given of a recently developed triangular equilibrium element which is then applied, in conjunction with the complementary energy principle, to the finite element analysis of some plate bending problems. The element is demonstrated to have a straightforward and satisfactory application and to possess advantages over the conventional triangular displacement element.

## 1. Introduction

A recent paper<sup>1</sup> provides the main details of a new element of triangular shape for the finite element analysis of plate bending problems. This element strictly satisfies all the equilibrium conditions between adjacent elements and is used in conjunction with the complementary energy principle. Certain details of this element are taken from the analogous plane stress analysis of Fraeijs de Veubeke<sup>2</sup> who, along with Argyris<sup>3</sup>, considers a displacement triangular element with linearly varying strain.

The book by Zienkiewicz<sup>4</sup> provides a useful account of previous work on the finite element method in the solution of plate bending problems. Briefly, the early research was directed towards displacement elements of rectangular shape which are non-conforming, *i.e.* they satisfy only partially the required kinematic conditions between adjacent elements. Although discussion prevails as to the assuredness of convergence with the use of such elements, they have nevertheless provided many useful results in actual applications. More recently, and under the stimulus of the need to deal with irregularly shaped boundaries, there has been developed the triangular displacement element, both of the non-conforming and conforming varieties. The latter element, in conjunction with the potential energy principle, provides assuredness of convergence. Unfortunately, however, this conforming displacement element is more complicated to use and, as Zienkiewicz<sup>4</sup> notes, it does not generally provide such a good approximation as the corresponding non-conforming element. In contrast, the present element, which strictly satisfies all the equilibrium conditions, is found here to have a straightforward and satisfactory application.

The paper commences with a recapitulation of the basic equations and limitation principle and goes on to provide a more detailed account of the finite element process which includes explicit expressions for the normal bending moment,

---

Received July 1967.

May 1968

149

Kirchhoff normal force and twisting moment which act at the boundary of the plate. In order to apply such statical boundary conditions it is necessary to impose their relative constraints during the variational procedure and an Appendix illustrates how these Lagrangian type constraints may be applied without increasing the order and without necessarily destroying the banded character of the flexibility matrix. Numerical results are then provided for a number of simple test problems and comparisons are made with results from displacement elements. While the present equilibrium element provides a remarkably good accuracy, it should be borne in mind, when making comparisons with the corresponding displacement element, where the order of the square  $K$  matrix is  $3N$  (with  $N$  the number of nodes), that the order of  $K$  is now equal to, or less than,  $3N+3T$  (where  $T$  is the number of triangles).

There are occasionally over-enthusiastic applications of the finite element method to problems which are not really suitable for such direct treatment. The final numerical application which is made here is intended to provide such an illustration; it concerns the difficult problem of a simply-supported square plate under uniformly distributed load where there is a concentric square hole with free edges. There is singular behaviour in the bending moments at the internal corners and the finite element solution now displays appreciable discontinuities in the distribution of bending moments, even away from the internal corner points. It is clear that such problems merit further attention, although it may be appropriate to recall that large discontinuities in the bending moment distribution occur in the application of the triangular displacement element to most problems.

### Notation

$A$	area of triangular finite element
$c, c_1, c_2$	arbitrary constants, see equation (4)
$C$	contour surrounding the region
$D$	flexural rigidity
$g$	column matrix, see equation (30)
$g'$	column matrix, see equation (38)
$H$	concentrated normal force acting at the boundary $C$ , see equation (10)
$H^*$	prescribed value of $H$
$I$	positive constant, see equation (45)
$K$	square flexibility matrix
$L$	length of side of square plate
$M_n, M_{ns}$	bending and twisting moments acting at the boundary $C$
$M_n^*$	prescribed value of $M_n$
$M_x, M_y, M_{xy}$	bending and twisting moments of the $xOy$ coordinate system

$n$	outward pointing normal
$N$	$3 \times 12$ matrix, see equation (1)
$N_x, N_y, N_z$	$3 \times 12$ matrices, see equation (1)
$P$	intensity of concentrated load
$P_c$	component of the concentrated load
$q$	column matrix of nodal loads. Also denotes the intensity of applied normal load
$q_0$	intensity of uniform load
$Q_{Vi}$	$i^{\text{th}}$ element of the column matrix $Q_V$
$Q_{Vi}'$	$i^{\text{th}}$ element of the column matrix $Q_V'$
$Q_n$	normal shearing force
$Q_x, Q_y$	normal shearing forces
$R$	finite region occupied by the plate
$s$	distance measured along the boundary in the sense of the normal $n$ . The mean value is denoted by $\bar{s}$
$T$	affix to denote triangles
$U, V$	two functions defined on the boundary
$U_c, U_c'$	components of the functions $U, V$
$V_n$	Kirchhoff normal force
$V_n^*$	prescribed value of $V_n$
$w$	normal deflection
$w^*$	prescribed value of $w$
$W_i$	weight function, see equation (1)
$x, y$	rectangular Cartesian coordinates
$x_i, y_i$	coordinates of a vertex
$x_{oc}, y_{oc}, x_c, y_c$	coordinates defined on the boundary
$\gamma$	angle included by the normal $n$ and the $x$ axis
$\Delta$	$3 \times 3$ matrix defined for each element, see equation (1)
$\Delta_0, \Delta_x, \Delta_y, \Delta_z$ , etc.	$3 \times 3$ matrices defined for each element
$\epsilon$	column matrix, see equation (1)
$\nu$	Poisson's ratio
$\Omega, \Omega_1, \Omega_2$	loading parameters

A few additional symbols are used in the text; they are introduced.

- $n$  outward pointing normal from the boundary  $C$
- $N$   $3 \times 12$  matrix, see equation (21)
- $N_0, N_x, N_y$   $3 \times 12$  matrices, see equation (23)
- $P$  intensity of concentrated normal load
- $P_C$  component of the complementary energy
- $q$  column matrix of generalised displacements, see equation (21). Also denotes the intensity of the distributed loading which is applied normal to the surface of the plate
- $q_0$  intensity of uniformly distributed load
- $Q_{vi}$   $i^{\text{th}}$  element of the column matrix  $g$ , see equations (31) and (32)
- $Q_{vi}'$   $i^{\text{th}}$  element of the column matrix  $g'$ , see equations (39) and (40)
- $Q_n$  normal shearing force acting at the boundary  $C$
- $Q_x, Q_y$  normal shearing forces of the  $xOy$  coordinate system
- $R$  finite region occupied by the plate
- $s$  distance measured around the boundary  $C$  in the clockwise sense. The meaning of  $s$  is changed for the purpose of Section 4
- $T$  affix to denote that the transpose is to be taken
- $U, V$  two functions defined by equations (1)
- $U_c, U_c'$  components of the complementary energy
- $V_n$  Kirchhoff normal force acting at the boundary  $C$
- $V_n^*$  prescribed value of  $V_n$
- $w$  normal deflection
- $w^*$  prescribed value of  $w$
- $W_i$  weight function, see equation (17)
- $x, y$  rectangular Cartesian coordinates
- $x_i, y_i$  coordinates of a vertex of the triangular finite element
- $x_{oc}, y_{oc}, x_c, y_c$  coordinates defined by Fig. 3
- $\gamma$  angle included by the intersection of the  $Ox$  axis with the normal  $n$
- $\Delta$   $3 \times 3$  matrix defining the flexibility characteristics of the finite element, see equation (24)
- $\Delta_0, \Delta_x$ , etc.  $3 \times 3$  matrices defined by equations (27)
- $\epsilon$  column matrix, see equation (20)
- $\nu$  Poisson's ratio
- $\Omega, \Omega_1, \Omega_2$  loading parameters, see equations (2) and (3)

A few additional symbols are used in the Appendix, but these are defined as they are introduced.

2. Basic Equations

In the earlier paper<sup>1</sup> it is noted that the equations of elemental equilibrium are satisfied if the moments and normal shearing forces are calculated from the two functions  $U(x, y)$  and  $V(x, y)$  such that

$$\left. \begin{aligned} M_x &= \frac{\partial V}{\partial y} - \Omega_1, & M_y &= \frac{\partial U}{\partial x} - \Omega_2, & M_{xy} &= \frac{1}{2} \left( \frac{\partial U}{\partial y} + \frac{\partial V}{\partial x} \right) \\ Q_x &= -\frac{1}{2} \frac{\partial}{\partial y} \left( \frac{\partial U}{\partial y} - \frac{\partial V}{\partial x} \right) - \frac{\partial \Omega_1}{\partial x}, & Q_y &= \frac{1}{2} \frac{\partial}{\partial x} \left( \frac{\partial U}{\partial y} - \frac{\partial V}{\partial x} \right) - \frac{\partial \Omega_2}{\partial y}. \end{aligned} \right\} \quad (1)$$

The two functions  $\Omega_1(x, y)$  and  $\Omega_2(x, y)$  may be chosen in any convenient way to satisfy the equation

$$q(x, y) = \frac{\partial^2 \Omega_1}{\partial x^2} + \frac{\partial^2 \Omega_2}{\partial y^2}, \quad (2)$$

where  $q$  represents the distribution of the loading which is applied normal to the surface of the plate. There are, however, some algebraic simplifications if it is stipulated that

$$\Omega_1 = \Omega_2 = \Omega \quad (\text{say}) \quad (3)$$

and this is adopted in the sequel since it involves no loss in generality. It is seen that any solution for  $U$  and  $V$  may be compounded with the functions

$$U = cy + c_1, \quad V = -cx + c_2, \quad (4)$$

where  $c_1, c_2$  and  $c$  are arbitrary constants.

The plate is considered to occupy a region denoted by  $R$  and is bounded by the contour  $C$ . The outward pointing normal is denoted by  $n$ ; the distance around  $C$  is measured in the clockwise sense by  $s$  (see Fig. 1), while the intersection of the normal  $n$  with the  $Ox$  axis includes the angle  $\gamma$ . On the boundary  $C$  it is usually more convenient to work in terms of the quantities  $M_n, M_{ns}$  and  $Q_n$ , which are respectively the normal bending moment, twisting moment and shearing force acting at the boundary.

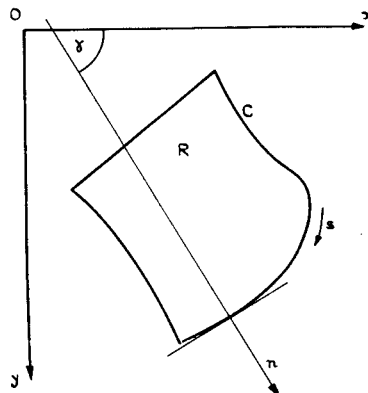


Figure 1. Notation for flat plate.

It can be shown that

$$\begin{aligned} M_n &= -\sin \gamma \frac{\partial U}{\partial s} + \cos \gamma \frac{\partial V}{\partial s} - \Omega \\ M_{ns} &= \frac{1}{2} \left( \cos \gamma \frac{\partial U}{\partial s} - \sin \gamma \frac{\partial U}{\partial n} + \sin \gamma \frac{\partial V}{\partial s} + \cos \gamma \frac{\partial V}{\partial n} \right) \\ Q_n &= -\frac{1}{2} \frac{\partial}{\partial s} \left( \cos \gamma \frac{\partial U}{\partial s} + \sin \gamma \frac{\partial U}{\partial n} - \sin \gamma \frac{\partial V}{\partial s} + \cos \gamma \frac{\partial V}{\partial n} \right) \end{aligned}$$

The Kirchhoff normal force is given by

$$V_n = Q_n - \frac{\partial M_{ns}}{\partial s} = -$$

The boundary value problem of  $C$  of one of the following pairs of

$$\begin{aligned} w &= w^* & \text{with} \\ w &= w^* & \text{with} \end{aligned}$$

$$\partial w / \partial n = \partial w^* / \partial n \quad \text{with}$$

$$-\sin \gamma \frac{\partial U}{\partial s} + \cos \gamma \frac{\partial V}{\partial s} = M_n^* \quad \text{with}$$

where the star (\*) denotes that the value is found convenient to put

$$M_n^* = M_n$$

At the corner points of  $C$ , and with  $H^*(s)$  is applied on  $C$ , then

$$\text{where} \quad H(s) = \int_{s^-}^{s^+} V_n ds =$$

In the finite element process principle

where, for an isotropic plate,

$$U_c = \frac{1}{2} \iint_R \frac{1}{(1-\nu^2)D} \left\{ \left( \frac{\partial U}{\partial x} \right)^2 + \left( \frac{\partial U}{\partial y} \right)^2 \right. + \left. 2\nu \frac{\partial U}{\partial x} \frac{\partial U}{\partial y} \right\} dx dy$$

It can be shown that

$$\left. \begin{aligned} M_n &= -\sin \gamma \frac{\partial U}{\partial s} + \cos \gamma \frac{\partial V}{\partial s} - \Omega \\ M_{ns} &= \frac{1}{2} \left( \cos \gamma \frac{\partial U}{\partial s} - \sin \gamma \frac{\partial U}{\partial n} + \sin \gamma \frac{\partial V}{\partial s} + \cos \gamma \frac{\partial V}{\partial n} \right) \\ Q_n &= -\frac{1}{2} \frac{\partial}{\partial s} \left( \cos \gamma \frac{\partial U}{\partial s} + \sin \gamma \frac{\partial U}{\partial n} + \sin \gamma \frac{\partial V}{\partial s} - \cos \gamma \frac{\partial V}{\partial n} \right) - \frac{\partial \Omega}{\partial n} \end{aligned} \right\} \quad (5)$$

The Kirchhoff normal force is given by

$$V_n = Q_n - \frac{\partial M_{ns}}{\partial s} = -\frac{\partial}{\partial s} \left( \cos \gamma \frac{\partial U}{\partial s} + \sin \gamma \frac{\partial V}{\partial s} \right) - \frac{\partial \Omega}{\partial n} \quad (6)$$

The boundary value problem normally requires the satisfaction on each part of  $C$  of one of the following pairs of conditions

$$\left. \begin{aligned} w &= w^* && \text{with} && \frac{\partial w}{\partial n} = \frac{\partial w^*}{\partial n} \\ w &= w^* && \text{with} && -\sin \gamma \frac{\partial U}{\partial s} + \cos \gamma \frac{\partial V}{\partial s} = M_n^* \\ \frac{\partial w}{\partial n} &= \frac{\partial w^*}{\partial n} && \text{with} && -\frac{\partial}{\partial s} \left( \cos \gamma \frac{\partial U}{\partial s} + \sin \gamma \frac{\partial V}{\partial s} \right) = V_n^* \\ -\sin \gamma \frac{\partial U}{\partial s} + \cos \gamma \frac{\partial V}{\partial s} &= M_n^* && \text{with} && -\frac{\partial}{\partial s} \left( \cos \gamma \frac{\partial U}{\partial s} + \sin \gamma \frac{\partial V}{\partial s} \right) = V_n^* \end{aligned} \right\} \quad (7)$$

where the star (\*) denotes that the quantity is completely prescribed and where it is found convenient to put

$$M_n^* = M_n + \Omega, \quad V_n^* = V_n + \frac{\partial \Omega}{\partial n} \quad (8)$$

At the corner points of  $C$ , and wherever a concentrated normal force of intensity  $H^*(s)$  is applied on  $C$ , then

$$H^*(s) = H(s), \quad (9)$$

where

$$H(s) = \int_{s^-}^{s^+} V_n ds = - \left[ \cos \gamma \frac{\partial U}{\partial s} + \sin \gamma \frac{\partial V}{\partial s} \right]_{s^-}^{s^+} \quad (10)$$

In the finite element process recourse is made to the complementary energy principle

$$\delta U_c + \delta U_c' + \delta P_c = 0 \quad (11)$$

where, for an isotropic plate,

$$U_c = \frac{1}{2} \int \int_R \frac{1}{(1-\nu^2)D} \left\{ \left( \frac{\partial U}{\partial x} \right)^2 + \left( \frac{\partial V}{\partial y} \right)^2 - 2\nu \frac{\partial U}{\partial x} \frac{\partial V}{\partial y} + \frac{(1+\nu)}{2} \left( \frac{\partial U}{\partial y} + \frac{\partial V}{\partial x} \right)^2 \right\} dx dy \quad (12)$$

ions of elemental equilibrium are  
ces are calculated from the two

$$\left. \begin{aligned} \left( \frac{\partial U}{\partial y} + \frac{\partial V}{\partial x} \right) \\ \left( \frac{\partial U}{\partial y} - \frac{\partial V}{\partial x} \right) - \frac{\partial \Omega_2}{\partial y} \end{aligned} \right\} \quad (1)$$

e chosen in any convenient way

$$\frac{\partial \Omega_2}{\partial y} \quad (2)$$

g which is applied normal to the  
algebraic simplifications if it is

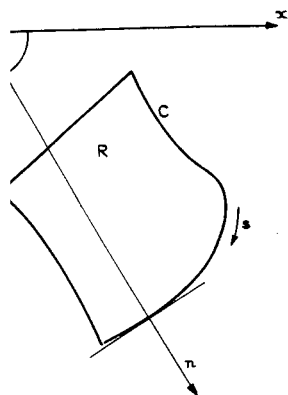
$$\quad (3)$$

s no loss in generality. It is seen  
ided with the functions

$$cx + c_2, \quad (4)$$

denoted by  $R$  and is bounded by  
lenoted by  $n$ ; the distance around  
g. 1), while the intersection of the

On the boundary  $C$  it is usually  
ities  $M_n$ ,  $M_{ns}$  and  $Q_n$ , which are  
moment and shearing force acting



The Aeronautical Quarterly

$$U_c' = \int \int_R \frac{1}{(1+\nu)D} \left\{ \Omega^2 - \Omega \left( \frac{\partial U}{\partial x} + \frac{\partial V}{\partial y} \right) \right\} dx dy \quad (13)$$

and

$$P_c = \int_C \left\{ \frac{\partial w^*}{\partial n} M_n - w^* V_n \right\} ds - \left[ w^* H(s) \right]_{s^-}^{s^+}, \quad (14)$$

where the expression in square brackets is evaluated at each corner point. In equations (12) to (14),  $\nu$  is the Poisson's ratio and  $D$  is the flexural rigidity, both of which may be (smooth) functions of the planar coordinates. It is to be noted, furthermore, that

$$\delta \Omega = 0 \quad (15)$$

and that on the boundary  $C$  it is necessary for the  $U, V$  fields to conform with the tractions  $M_n, V_n$  and  $H$ , wherever they are prescribed, before commencing the variational process. In virtue of the fact that a complementary energy principle is employed it is known that the strain energy enjoys the following limitation principle

$$\text{strain energy} \leq U_c + U_c', \quad (16)$$

whenever  $P_c = 0$ , as is the case for homogeneous kinematic boundary conditions.

### 3. The Finite Element Process

It is now assumed that the region  $R$  is subdivided into a number of finite triangular elements and this implies that a curved boundary  $C$  is approximated by straight line segments. A typical element is shown in Fig. 2, where the vertices of the triangle, *i.e.* the nodes, are numbered 1, 2, 3 in the positive sense of  $s$  while the mid-points of the sides are numbered 1', 2', 3'. Both  $U$  and  $V$  in each triangle

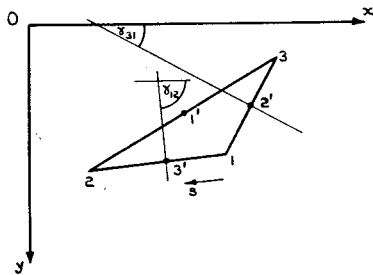


Figure 2. Notation for triangular finite element.

are taken to be general quadratic expressions in the rectangular coordinates. Along an edge of the triangle they both vary according to a parabolic law and are here completely specified by their values at three points along the edge. Accordingly, a suitable choice of the generalised coordinates is the twelve values of  $U$  and  $V$  at the vertices and at the mid-points of the edges. Thus, in accord with the work of Fraeijs de Veubeke<sup>2</sup> for the analogous plane stress problem,

$$\left. \begin{aligned} U(x, y) &= U_1 W_1 + U_2 W_2 + U_3 W_3 + U_{1'} W_{1'} + U_{2'} W_{2'} + U_{3'} W_{3'} \\ V(x, y) &= V_1 W_1 + V_2 W_2 + V_3 W_3 + V_{1'} W_{1'} + V_{2'} W_{2'} + V_{3'} W_{3'} \end{aligned} \right\} \quad (17)$$

The weight functions  $W_1(x, y)$ , etc. in the earlier paper<sup>1</sup>. Moreover, along the

$$U(s) = U_1 - \frac{s-s_1}{s_2-s_1} (3U_1 + U_2 - 4U_{1'})$$

$$V(s) = V_1 - \frac{s-s_1}{s_2-s_1} (3V_1 + V_2 - 4V_{1'})$$

Equations (17) ensure the continuity of the normal bending moment across the finite element boundaries like  $H$  (see equation (10)), at the upper row matrix

$$q^T = (U_1, U_2, U_3, U_{1'}, U_{2'}, U_{3'})$$

and by  $\epsilon^T$  the row matrix  $\epsilon^T =$

we can write the matrix equation

where the elements of the  $3 \times 12$  matrix are the derivatives of the weight functions  $W_1(x, y)$

We now introduce the matrix

where  $R_{123}$  denotes the region occupied by the element. In the course of numerical calculation it is convenient to convert the

$$2A^2 \Delta$$

where the matrices  $N_0, N_x$  and  $N_y$  are defined for the triangular element is denoted by

$$\Delta = \frac{1}{(1-\nu^2)D} \int_{R_{123}} dx dy$$

We can now write the matrix  $K$  of the element

$$K = \frac{1}{4A^4} (N_0^T \Delta_0 N_0 + N_x^T \Delta_x N_x + N_y^T \Delta_y N_y + N_x^T \Delta_x N_y + N_y^T \Delta_y N_x)$$

where  $\Delta_0 = \int \int_{R_{123}} \Delta dx dy$

The weight functions  $W_1(x, y)$ , etc. are quadratic in  $x$  and  $y$  and are given in the earlier paper<sup>1</sup>. Moreover, along the edge 1, 3', 2 of the triangle shown in Fig. 2,

$$\left. \begin{aligned} U(s) &= U_1 - \frac{s-s_1}{s_2-s_1} (3U_1 + U_2 - 4U_{3'}) + 2 \left( \frac{s-s_1}{s_2-s_1} \right)^2 (U_1 + U_2 - 2U_{3'}) \\ V(s) &= V_1 - \frac{s-s_1}{s_2-s_1} (3V_1 + V_2 - 4V_{3'}) + 2 \left( \frac{s-s_1}{s_2-s_1} \right)^2 (V_1 + V_2 - 2V_{3'}) \end{aligned} \right\} \quad (18)$$

Equations (17) ensure the continuity of both  $U$  and  $V$  throughout  $R$  and the continuity of the normal bending moment  $M_n$  and the Kirchhoff normal force  $V_n$  across the finite element boundaries, as well as the vanishing of concentrated forces like  $H$  (see equation (10)), at the unions of nodes inside  $R$ . Let us denote by  $q^T$  the row matrix

$$q^T = (U_1, U_2, U_3, U_{1'}, U_{2'}, U_{3'}, V_1, V_2, V_3, V_{1'}, V_{2'}, V_{3'}) \quad (19)$$

and by  $\epsilon^T$  the row matrix 
$$\epsilon^T = \left( \frac{\partial U}{\partial x}, \frac{\partial V}{\partial y}, \frac{\partial U}{\partial y} + \frac{\partial V}{\partial x} \right); \quad (20)$$

we can write the matrix equation 
$$\epsilon = Nq, \quad (21)$$

where the elements of the  $3 \times 12$  matrix  $N$  are calculated from the partial derivatives of the weight functions  $W_1(x, y)$  after their substitution into equations (17).

We now introduce the matrix 
$$K = \int \int_{R_{123}} (N^T \Delta N) dx dy, \quad (22)$$

where  $R_{123}$  denotes the region occupied by the triangular element. For the purpose of numerical calculation it is convenient to expand the  $N$  matrix in the form

$$2A^2 N = N_0 + xN_x + yN_y, \quad (23)$$

where the matrices  $N_0$ ,  $N_x$  and  $N_y$  have constant elements and where the area of the triangular element is denoted by  $A$ . For an isotropic element the matrix  $\Delta$  is

$$\Delta = \frac{1}{(1-\nu^2)D(x, y)} \begin{bmatrix} 1 & -\nu & 0 \\ -\nu & 1 & 0 \\ 0 & 0 & \frac{1+\nu}{2} \end{bmatrix}. \quad (24)$$

We can now write the matrix  $K$  of equation (22) in the form

$$K = \frac{1}{4A^4} (N_0^T \Delta_0 N_0 + N_0^T \Delta_x N_x + N_x^T \Delta_x N_0 + N_0^T \Delta_y N_y + N_y^T \Delta_y N_0 + N_x^T \Delta_{xx} N_x + N_x^T \Delta_{xy} N_y + N_y^T \Delta_{xy} N_x + N_y^T \Delta_{yy} N_y), \quad (25)$$

where 
$$\Delta_0 = \int \int_{R_{123}} \Delta dx dy, \quad \Delta_x = \int \int_{R_{123}} \Delta x dx dy, \quad \text{etc.} \quad (26)$$

$$\left. \frac{\partial V}{\partial y} \right\} dx dy \quad (13)$$

$$H(s) \Big|_{s^-}^{s^+}, \quad (14)$$

ed at each corner point. In is the flexural rigidity, both of ordinates. It is to be noted,

$$(15)$$

,  $V$  fields to conform with the before commencing the varia- elementary energy principle is following limitation principle

$$(16)$$

nematic boundary conditions.

vided into a number of finite boundary  $C$  is approximated by n Fig. 2, where the vertices of the positive sense of  $s$  while both  $U$  and  $V$  in each triangle

Notation for triangular finite element.

rectangular coordinates. Along a parabolic law and are here along the edge. Accordingly, the twelve values of  $U$  and  $V$  us, in accord with the work of elem,

$$\left. \begin{aligned} U_2 W_2 + U_3 W_3 \\ V_2 W_2 + V_3 W_3 \end{aligned} \right\}. \quad (17)$$

The element of constant flexural rigidity is of especial technological importance and in this case  $\Delta$  is a matrix of constants where, after a preliminary shift of the rectangular co-ordinates to the centre of area of the element, we have

$$\left. \begin{aligned} \Delta_0 &= A\Delta, & \Delta_x &= \Delta_y = 0, & \Delta_{xx} &= (x_1^2 + x_2^2 + x_3^2) A\Delta/12 \\ \Delta_{xy} &= (x_1y_1 + x_2y_2 + x_3y_3) A\Delta/12, & \Delta_{yy} &= (y_1^2 + y_2^2 + y_3^2) A\Delta/12. \end{aligned} \right\} \quad (27)$$

We can now write  $\delta U_c$  of equation (11) in the form

$$\delta U_c = \frac{\delta}{2} \int \int_{R_{123}} (\epsilon^T \Delta \epsilon) dx dy = \delta q^T K q. \quad (28)$$

In calculating the variation  $\delta U_c'$  (see equations (11) and (13)) we may, in virtue of equation (15), neglect the term in  $\Omega^2$ . Thus, in matrix notation

$$\delta U_c' = -g^T \delta q, \quad (29)$$

where  $g^T$  is the row matrix

$$g^T = (Q_{U1}, Q_{U2}, Q_{U3}, Q_{U1'}, Q_{U2'}, Q_{U3'}, Q_{V1}, Q_{V2}, Q_{V3}, Q_{V1'}, Q_{V2'}, Q_{V3'}) \quad (30)$$

with the  $Q_U$  calculated from 
$$\int \int_{R_{123}} \frac{1}{(1+\nu)D} \Omega \frac{\partial U}{\partial x} dx dy \quad (31)$$

on substituting for  $U$  from the first of equations (17) and the  $Q_V$  from

$$\int \int_{R_{123}} \frac{1}{(1+\nu)D} \Omega \frac{\partial V}{\partial y} dx dy \quad (32)$$

on substituting for  $V$  from the second of equations (17). Both equations (31) and (32) need to be modified when the triangular element is other than isotropic. In the special case of a uniformly distributed load of unit intensity we may put

$$\Omega = (x^2 + y^2)/4 \quad (33)$$

and in the evaluation of equations (31) and (32) it is useful to note, after shifting the rectangular coordinates to the centre of area of the element, that

$$\left. \begin{aligned} \int \int_{R_{123}} x^3 dx dy &= \frac{A}{10} x_1 x_2 x_3, & \int \int_{R_{123}} x^2 y dx dy &= \frac{A}{30} (x_1 x_2 y_3 + x_2 x_3 y_1 + x_1 x_3 y_2) \\ \int \int_{R_{123}} y^3 dx dy &= \frac{A}{10} y_1 y_2 y_3, & \int \int_{R_{123}} x y^2 dx dy &= \frac{A}{30} (x_1 y_2 y_3 + x_2 y_1 y_3 + x_3 y_1 y_2). \end{aligned} \right\} \quad (34)$$

For a concentrated load, however, the expression for  $\Omega$  is logarithmic and it is probably better then to perform the corresponding quadratures numerically.

The variation  $\delta P_c$  (see equation 2 of the element shown in Fig. 2)  $V_n$  and  $H(s)$  from equations (5) becomes

$$\delta P_c = \int_{s_1}^{s_2} \left\{ \frac{\partial w^*}{\partial n} \left( -\sin \gamma_{12} \frac{\partial \delta U}{\partial s} + \cos \gamma_{12} \right) \right.$$

which, after an integration by parts,

$$\delta P_c = \int_{s_1}^{s_2} \left\{ \frac{\partial w^*}{\partial n} \left( -\sin \gamma_{12} \frac{\partial \delta U}{\partial s} + \cos \gamma_{12} \right) \right.$$

The evaluation of this equation is similar to that of equation (31) and (32)

$$\begin{aligned} \frac{\partial \delta U}{\partial s} &= -\frac{1}{s_2 - s_1} (3\delta U_1 + \delta U_2) \\ \frac{\partial \delta V}{\partial s} &= -\frac{1}{s_2 - s_1} (3\delta V_1 + \delta V_2) \end{aligned}$$

In the numerical examples which are evaluated with the aid of Simpson's rule, values of  $\partial w^*/\partial n$  and  $\partial w^*/\partial s$  at the convenient, it is based upon a quadratic representation of  $s$ , whereas a cubic representation is used for  $s$ , write

where  $g'^T$  is the row matrix

$$g'^T = (Q_{U1'}, Q_{U2'}, Q_{U3'}, Q_{U1''), Q_{U2''), Q_{U3''), Q_{V1'}, Q_{V2'}, Q_{V3'})$$

with the  $Q_{U'}$  calculated from

$$\int_{s_1}^{s_2} \left( \sin \gamma_{12} \frac{\partial w^*}{\partial n} \right)$$

and the  $Q_{V'}$  from

$$\int_{s_1}^{s_2} \left( -\cos \gamma_{12} \frac{\partial w^*}{\partial s} \right)$$

especial technological importance  
 re, after a preliminary shift of the  
 e element, we have

$$\left. \begin{aligned} x &= (x_1^2 + x_2^2 + x_3^2) A\Delta/12 \\ y &= (y_1^2 + y_2^2 + y_3^2) A\Delta/12. \end{aligned} \right\} \quad (27)$$

$$= \delta q^T K q. \quad (28)$$

ms (11) and (13)) we may, in virtue  
 matrix notation

$$(29)$$

$$Q_{v_2}, Q_{v_3}, Q_{v_1}, Q_{v_2}, Q_{v_3}) \quad (30)$$

$$dx dy \quad (31)$$

7) and the  $Q_v$  from

$$dx dy \quad (32)$$

ons (17). Both equations (31) and  
 nent is other than isotropic. In the  
 t intensity we may put

$$(33)$$

t is useful to note, after shifting the  
 the element, that

$$\left. \begin{aligned} x_1 x_2 y_3 + x_2 x_3 y_1 + x_1 x_3 y_2 \\ x_1 y_2 y_3 + x_2 y_1 y_3 + x_3 y_1 y_2. \end{aligned} \right\} \quad (34)$$

ion for  $\Omega$  is logarithmic and it is  
 ing quadratures numerically.

The variation  $\delta P_c$  (see equations (11) and (14)) is null unless at least one side  
 of the triangular element is coincident with the boundary  $C$ . Let the vertices 1 and  
 2 of the element shown in Fig. 2 coincide with  $C$  so that, on substituting for  $M_n$ ,  
 $V_n$  and  $H(s)$  from equations (5), (6) and (10), the variation of equation (14)  
 becomes

$$\delta P_c = \int_{s_1}^{s_2} \left\{ \frac{\partial w^*}{\partial n} \left( -\sin \gamma_{12} \frac{\partial \delta U}{\partial s} + \cos \gamma_{12} \frac{\partial \delta V}{\partial s} \right) + w^* \frac{\partial}{\partial s} \left( \cos \gamma_{12} \frac{\partial \delta U}{\partial s} + \sin \gamma_{12} \frac{\partial \delta V}{\partial s} \right) \right\} ds - \left[ w^* \left( \cos \gamma_{12} \frac{\partial \delta U}{\partial s} + \sin \gamma_{12} \frac{\partial \delta V}{\partial s} \right) \right]_{s_1}^{s_2}$$

which, after an integration by parts, becomes

$$\delta P_c = \int_{s_1}^{s_2} \left\{ \frac{\partial w^*}{\partial n} \left( -\sin \gamma_{12} \frac{\partial \delta U}{\partial s} + \cos \gamma_{12} \frac{\partial \delta V}{\partial s} \right) - \frac{\partial w^*}{\partial s} \left( \cos \gamma_{12} \frac{\partial \delta U}{\partial s} + \sin \gamma_{12} \frac{\partial \delta V}{\partial s} \right) \right\} ds. \quad (35)$$

The evaluation of this equation is simplified by noting that equation (18) provides

$$\left. \begin{aligned} \frac{\partial \delta U}{\partial s} &= -\frac{1}{s_2 - s_1} (3\delta U_1 + \delta U_2 - 4\delta U_3) + \frac{4(s - s_1)}{(s_2 - s_1)^2} (\delta U_1 + \delta U_2 - 2\delta U_3) \\ \frac{\partial \delta V}{\partial s} &= -\frac{1}{s_2 - s_1} (3\delta V_1 + \delta V_2 - 4\delta V_3) + \frac{4(s - s_1)}{(s_2 - s_1)^2} (\delta V_1 + \delta V_2 - 2\delta V_3). \end{aligned} \right\} \quad (36)$$

In the numerical examples which are treated later, the quadratures of equation (35)  
 are evaluated with the aid of Simpson's rule by considering only the prescribed  
 values of  $\partial w^*/\partial n$  and  $\partial w^*/\partial s$  at the points 1, 3' and 2. (Although this is very con-  
 venient, it is based upon a quadratic representation of the integrand between  $s_1$  and  
 $s_2$ , whereas a cubic representation is strictly required.) Thus, in matrix notation we  
 write

$$\delta P_c = -g^T \delta q, \quad (37)$$

where  $g^T$  is the row matrix

$$g^T = (Q_{u_1'}, Q_{u_2'}, Q_{u_3'}, Q_{u_1'}, Q_{u_2'}, Q_{u_3'}, Q_{v_1'}, Q_{v_2'}, Q_{v_3'}, Q_{v_1'}, Q_{v_2'}, Q_{v_3}'), \quad (38)$$

with the  $Q_{u'}$  calculated from

$$\int_{s_1}^{s_2} \left( \sin \gamma_{12} \frac{\partial w^*}{\partial n} + \cos \gamma_{12} \frac{\partial w^*}{\partial s} \right) \frac{\partial U}{\partial s} ds \quad (39)$$

and the  $Q_{v'}$  from

$$\int_{s_1}^{s_2} \left( -\cos \gamma_{12} \frac{\partial w^*}{\partial n} + \sin \gamma_{12} \frac{\partial w^*}{\partial s} \right) \frac{\partial V}{\partial s} ds. \quad (40)$$

In terms of the generalised quantities the complementary energy principle of equation (11) now requires that

$$\delta q^T (Kq - g - g') = 0 \tag{41}$$

(see equations (28), (29) and (37)). It is remarked that the  $K$  matrix, which is assembled with the contributions from all the triangular elements in  $R$ , is usually banded along the leading diagonal and that the variations of the row matrix  $\delta q^T$  are subjected to certain constraints. Thus, in view of the arbitrariness of  $U$  and  $V$  as expressed by equations (4), it is always necessary to fix three values of  $U$  or  $V$  (at least one of each) as if to restrict the rigid body movements of the same plate under plane stress. Furthermore, it is necessary for the  $U, V$  fields to conform with the tractions  $M_n, V_n$  and  $H$  wherever they are prescribed on the boundary  $C$ . Thus, for the triangular element shown in Fig. 2 where the vertices 1 and 2 are taken to coincide with  $C$ , we have, on substituting equation (18) into the appropriate parts of equations (7),

$$\left. \begin{aligned} (3U_1 + U_2 - 4U_3) \sin \gamma_{12} - (3V_1 + V_2 - 4V_3) \cos \gamma_{12} &= (s_2 - s_1) M_n^*(s_1) \\ -(U_1 + 3U_2 - 4U_3) \sin \gamma_{12} + (V_1 + 3V_2 - 4V_3) \cos \gamma_{12} &= (s_2 - s_1) M_n^*(s_2) \\ -4(U_1 + U_2 - 2U_3) \cos \gamma_{12} - 4(V_1 + V_2 - 2V_3) \sin \gamma_{12} &= (s_2 - s_1)^2 V_n^*(s_3), \end{aligned} \right\} \tag{42}$$

where it is understood that the prescribed distribution of  $M_n^*(s)$  between  $s_1$  and  $s_2$  is approximated by the best linear fit, and the prescribed distribution of  $V_n^*(s)$  by the best constant fit. Suppose now that a concentrated force  $H^*(s_1)$  is applied at vertex 1 and assume for the present illustrative purpose that the edge 3, 2', 1 also coincides with  $C$ , then equations (9) and (10) show that

$$\frac{1}{s_1 - s_3} \{ (U_3 + 3U_1 - 4U_2) \cos \gamma_{31} + (V_3 + 3V_1 - 4V_2) \sin \gamma_{31} \} + \frac{1}{s_2 - s_1} \{ (3U_1 + U_2 - 4U_3) \cos \gamma_{12} + (3V_1 + V_2 - 4V_3) \sin \gamma_{12} \} = H^*(s_1). \tag{43}$$

The manner of dealing with these constraints upon the variations of equation (41) is dealt with in the Appendix, where it is pointed out that their imposition upon the variational process does not necessarily destroy the banded character of the calculations nor lead to the inversion of a matrix of higher order than  $K$ . There are occasions, moreover, such as when  $M_n, V_n$  and  $H$  are prescribed around only one singly connected part of  $C$ , when it is possible to solve the constraint equations explicitly for the boundary values of  $U$  and  $V$ . Finally, it is to be remembered that the boundary tractions must never be overprescribed, for it is recalled that the method of solution proceeds on the implicit basis that the overall equations of equilibrium are satisfied.

The use of the limitation principle of equation (16) is valuable when inspecting the "overall convergence" of the numerical solution on the basis of successive advances to finer networks of elemental triangles. This principle can be expressed in matrix notation (see equations (12), (13), (28) and (29)) as follows.

strain energy  $\leq \frac{1}{2} q^T$

where

$$I(\Omega^2) = \int$$

is an essentially positive constant qu advance to finer networks. In virtue however, it is noted that small errors limitation principle because of the representation reproduces a prescribed boundary  $C$ .

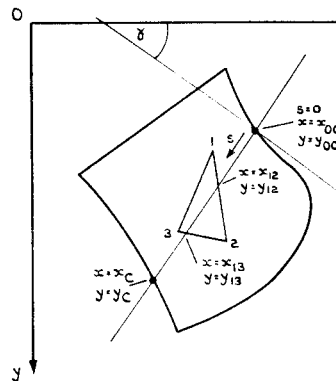
#### 4. Calculation of the Deflection

Once the numerical values of the finite element process described in the deflected shape  $w(x, y)$  of curvature relations which, for an isotro

$$\frac{\partial^2 w}{\partial x^2} = -\frac{1}{D(1-\nu^2)} (M_x - \nu M_y), \quad \frac{\partial^2 w}{\partial y^2} = -$$

However, in view of the (usually) app is provided by the finite element analy tion of these equations does not gener point—because this value is depende

Let us consider equations (46)  $(x_c, y_c)$  which passes through the regi it is convenient to change the meanir this straight line from its first intersec same way  $\gamma$  now denotes the angle wh to this straight line.



$$\text{strain energy} \leq \frac{1}{2} q^T K q - g^T q + I(\Omega^2), \tag{44}$$

where

$$I(\Omega^2) = \int \int_R \frac{\Omega^2}{(1+\nu)D} dx dy \tag{45}$$

is an essentially positive constant quantity which remains unchanged during the advance to finer networks. In virtue of the statement which follows equation (42), however, it is noted that small errors are liable to occur in the application of the limitation principle because of the restrictive manner in which the finite element representation reproduces a prescribed distribution of  $M_n^*(s)$  and  $V_n^*(s)$  on the boundary  $C$ .

**4. Calculation of the Deflection**

Once the numerical values of the moments  $M_x$ ,  $M_y$  and  $M_{xy}$  are calculated by the finite element process described in the previous section, it is possible to determine the deflected shape  $w(x, y)$  of the bent plate by integrating the moment-curvature relations which, for an isotropic element, are

$$\frac{\partial^2 w}{\partial x^2} = -\frac{1}{D(1-\nu^2)}(M_x - \nu M_y), \quad \frac{\partial^2 w}{\partial y^2} = -\frac{1}{D(1-\nu^2)}(M_y - \nu M_x), \quad \frac{\partial^2 w}{\partial x \partial y} = \frac{1}{D(1-\nu^2)} M_{xy}. \tag{46}$$

However, in view of the (usually) approximate character of  $M_x$ ,  $M_y$  and  $M_{xy}$  which is provided by the finite element analysis, it is noted that the straightforward integration of these equations does not generally provide a unique value of  $w$  at a specific point—because this value is dependent upon the chosen integration path.

Let us consider equations (46) along the straight line joining  $(x_{oc}, y_{oc})$  and  $(x_c, y_c)$  which passes through the region  $R$ , as shown in Fig. 3. For this purpose it is convenient to change the meaning of  $s$  so that it measures the distance along this straight line from its first intersection at  $(x_{oc}, y_{oc})$  with the boundary  $C$ ; in the same way  $\gamma$  now denotes the angle which is included by the  $Ox$  axis and the normal to this straight line.

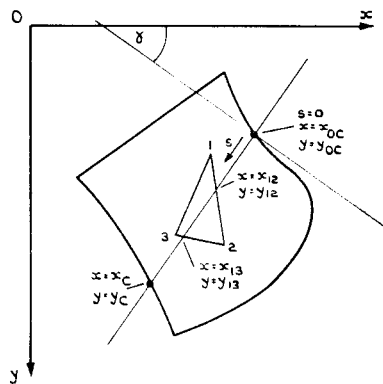


Figure 3. Notation for calculating the deflection.

complementary energy principle of  
=0 (41)

arked that the  $K$  matrix, which is  
angular elements in  $R$ , is usually  
variations of the row matrix  $\delta q^T$   
ew of the arbitrariness of  $U$  and  $V$   
essary to fix three values of  $U$  or  
body movements of the same plate  
for the  $U, V$  fields to conform with  
rescribed on the boundary  $C$ . Thus,  
re the vertices 1 and 2 are taken to  
tion (18) into the appropriate parts

$$\left. \begin{aligned} V_3 \cos \gamma_{12} &= (s_2 - s_1) M_n^*(s_1) \\ V_2 \cos \gamma_{12} &= (s_2 - s_1) M_n^*(s_2) \\ V_3 \sin \gamma_{12} &= (s_2 - s_1)^2 V_n^*(s_3), \end{aligned} \right\} \tag{42}$$

tribution of  $M_n^*(s)$  between  $s_1$  and  $s_2$   
e prescribed distribution of  $V_n^*(s)$   
oncentrated force  $H^*(s_1)$  is applied  
ative purpose that the edge 3, 2', 1  
) show that

$$V_2 \sin \gamma_{31} + V_2 - 4V_3 \sin \gamma_{12} = H^*(s_1). \tag{43}$$

upon the variations of equation (41)  
nted out that their imposition upon  
lestroy the banded character of the  
atrix of higher order than  $K$ . There  
n and  $H$  are prescribed around only  
ible to solve the constraint equations  
Finally, it is to be remembered that  
rescribed, for it is recalled that the  
basis that the overall equations of

ation (16) is valuable when inspecting  
solution on the basis of successive  
gles. This principle can be expressed  
(8) and (29)) as follows.

Taking note of the directional derivative

$$\frac{\partial w}{\partial s} = -\sin \gamma \frac{\partial w}{\partial x} + \cos \gamma \frac{\partial w}{\partial y}, \tag{47}$$

it follows, since  $\gamma$  is constant, that

$$\begin{aligned} \frac{\partial^2 w}{\partial s^2} &= \sin^2 \gamma \frac{\partial^2 w}{\partial x^2} + \cos^2 \gamma \frac{\partial^2 w}{\partial y^2} - 2 \sin \gamma \cos \gamma \frac{\partial^2 w}{\partial x \partial y} \\ &= -\frac{1}{D(1-\nu^2)} \{ M_x (\sin^2 \gamma - \nu \cos^2 \gamma) + M_y (\cos^2 \gamma - \nu \sin^2 \gamma) + \\ &\quad + 2(1+\nu) M_{xy} \sin \gamma \cos \gamma \}, \tag{48} \end{aligned}$$

after substituting from equations (46). A further substitution from equations (1) and (3) provides

$$\begin{aligned} \frac{\partial^2 w}{\partial s^2} &= -\frac{1}{D(1-\nu^2)} \left\{ -(1-\nu) \Omega + (\sin^2 \gamma - \nu \cos^2 \gamma) \frac{\partial V}{\partial y} + \right. \\ &\quad \left. + (\cos^2 \gamma - \nu \sin^2 \gamma) \frac{\partial U}{\partial x} + (1+\nu) \sin \gamma \cos \gamma \left( \frac{\partial U}{\partial y} + \frac{\partial V}{\partial x} \right) \right\}. \tag{49} \end{aligned}$$

In integrating this expression through the triangle 1, 2, 3, as shown in Fig. 3, it is useful to note that the intersection point  $(x_{12}, y_{12})$ , for example, is given by

$$\left. \begin{aligned} x_{12} &= \frac{(x_{oc} - x_c)(x_1 x_2 - x_2 y_1) - (x_1 - x_2)(x_{oc} y_c - x_c y_{oc})}{(x_1 - x_2)(y_{oc} - y_c) - (x_{oc} - x_c)(y_1 - y_2)} \\ y_{12} &= \frac{(y_{oc} - y_c)(x_1 y_2 - x_2 y_1) - (y_1 - y_2)(x_{oc} y_c - x_c y_{oc})}{(x_1 - x_2)(y_{oc} - y_c) - (x_{oc} - x_c)(y_1 - y_2)} \end{aligned} \right\} \tag{50}$$

and that there is only a linear variation in the quantities  $\partial U/\partial x$ ,  $\partial U/\partial y$ ,  $\partial V/\partial x$  and  $\partial V/\partial y$  along the straight line joining  $(x_{12}, y_{12})$  and  $(x_{23}, y_{23})$ . Furthermore, for the special case of a uniformly distributed load of unit intensity (see equation (33)), we have, along the straight line joining  $(x_{oc}, y_{oc})$  and  $(x_c, y_c)$ ,

$$4\Omega(s) = x_{oc}^2 + y_{oc}^2 - 2s(x_{oc} \sin \gamma - y_{oc} \cos \gamma) + s^2. \tag{51}$$

Finally, it is necessary for both  $w$  and  $\partial w/\partial s$  to be continuous along this line.

### 5. Numerical Examples

A few simple test problems are now computed to illustrate the accuracy and rate of convergence of our triangular equilibrium element and to obtain comparisons with corresponding results obtained from displacement elements. The final application concerns a simply-supported square plate under uniformly distributed load where there is a concentric square hole with free edges. The results from this problem serve to illustrate the consequences of direct application of finite element, and other similar techniques, to unsuitable problems. In all examples the Poisson's ratio is taken as  $\nu = 0.3$ .

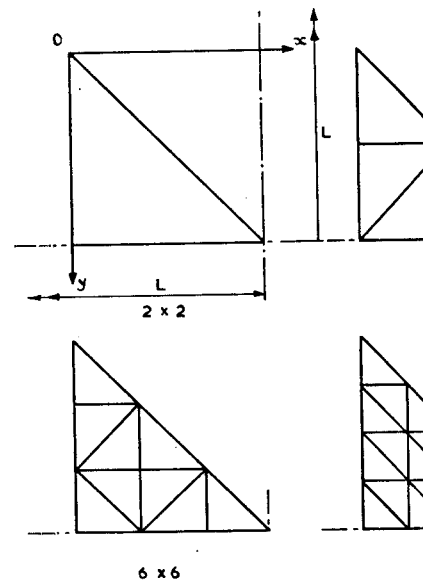


Figure 4. Square plate

The book by Zienkiewicz<sup>4</sup> provides analyses, especially for square isotropic. Although the results for non-conforming accurate than those provided by Zienkiewicz results are quoted here whenever they are an equilibrium analysis by providing the low is stored in the plate.

Because of the symmetry of the isotropic is either uniformly distributed of intensity load  $P$ , it is necessary only to consider where the various arrangements of triangles of Zienkiewicz. The rectangular coordinate centre of the plate (see Fig. 4) and run of all the uniformly distributed load equation (3) as

$$\Omega = q_0 ($$

Shortage of time has prevented the preparation of computer routines which are required for the computations are preceded here by the

$$w =$$

$$\text{where } r^2 =$$

PLATE BENDING

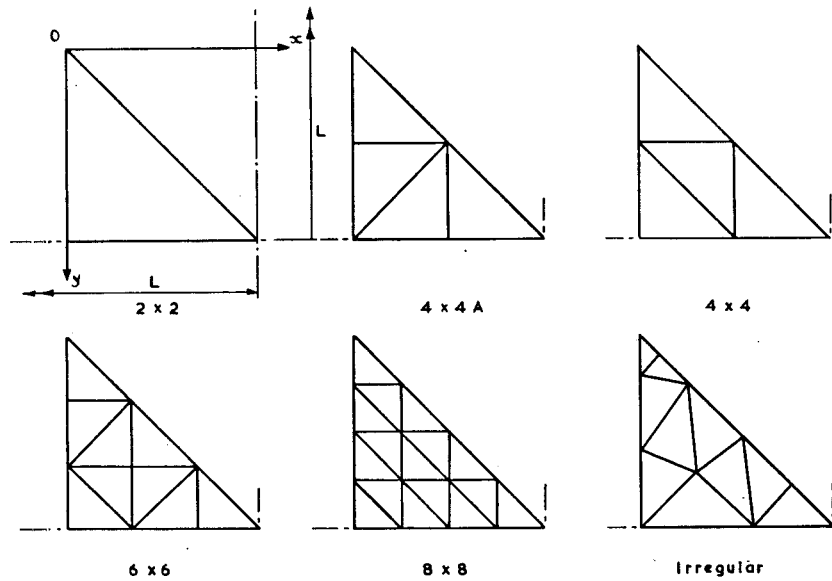


Figure 4. Square plate. Elemental divisions.

The book by Zienkiewicz<sup>4</sup> provides many interesting results of displacement analyses, especially for square isotropic plates with various boundary conditions. Although the results for non-conforming displacement elements are generally more accurate than those provided by Zienkiewicz for conforming elements, these latter results are quoted here whenever they are available, because they complement our equilibrium analysis by providing the lower bound to the actual strain energy which is stored in the plate.

Because of the symmetry of the isotropic square plate and the loading, which is either uniformly distributed of intensity  $q_0$  per unit area or a central concentrated load  $P$ , it is necessary only to consider the one-eighth portion as shown in Fig. 4 where the various arrangements of triangular element divisions are similar to those of Zienkiewicz. The rectangular coordinate axes  $xOy$  are always taken at the centre of the plate (see Fig. 4) and run parallel with the sides. For the purpose of all the uniformly distributed load calculations we take the quantity  $\Omega$  of equation (3) as

$$\Omega = q_0 (x^2 + y^2) / 4. \tag{52}$$

Shortage of time has prevented the preparation of the numerical integration computer routines which are required for the concentrated load case and so these computations are preceded here by the extraction of the particular solution

$$w = \frac{P}{8\pi D} r^2 \log r, \tag{53}$$

where  $r^2 = x^2 + y^2$ .

$$\dots \gamma \frac{\partial w}{\partial y}, \tag{47}$$

$$\dots \gamma - \nu \sin^2 \gamma) + \dots (1 + \nu) M_{xy} \sin \gamma \cos \gamma), \tag{48}$$

or substitution from equations (1)

$$\frac{\partial V}{\partial y} + \dots \sin \gamma \cos \gamma \left( \frac{\partial U}{\partial y} + \frac{\partial V}{\partial x} \right) \}. \tag{49}$$

e 1, 2, 3, as shown in Fig. 3, it is, for example, is given by

$$\left. \begin{aligned} & \frac{v_2}{-x_c} (x_{oc}y_c - x_c y_{oc}) \\ & \frac{v_2}{-x_c} (x_{oc}y_c - x_c y_{oc}) \end{aligned} \right\} \tag{50}$$

quantities  $\partial U / \partial x$ ,  $\partial U / \partial y$ ,  $\partial V / \partial x$  and  $(x_{23}, y_{23})$ . Furthermore, for unit intensity (see equation (33)),  $v_c$  and  $(x_c, y_c)$ ,

$$\dots - y_{oc} \cos \gamma) + s^2. \tag{51}$$

to be continuous along this line.

ited to illustrate the accuracy and element and to obtain comparisons ment elements. The final applica- under uniformly distributed load free edges. The results from this direct application of finite element, ms. In all examples the Poisson's

**TABLE I**  
SIMPLY-SUPPORTED SQUARE PLATE UNDER UNIFORMLY DISTRIBUTED LOAD

Mesh	Centre of side $V_y$	Centre of plate $M_x$ $M_y$		Corner reaction $ 2M_{xy} $	Strain energy $-I(\Omega^2)$ is less than (see equation (44))
	2x2	-0.309	0.0421	0.0300	0.068
4x4A	-0.310 (-0.370)	0.0470	0.0434	0.069	-0.00012667
4x4	-0.378	0.0470	0.0435	0.069	-0.00012658
6x6	-0.392	0.0475	0.0459	0.067	-0.00012717
8x8	-0.401	0.0477	0.0468	0.067	-0.00012725
irregular exact	-0.345 (-0.376)	0.0477	0.0477	0.070	-0.00012701
	-0.420	0.0479	0.0479	0.065	—
Multiplier	$q_0 L$	$q_0 L^2$	$q_0 L^2$	$q_0 L^2$	$8q_0^2 L^5 / D$

The alternative values, shown in parentheses, occur when the position coincides with the common vertex of two elements.

Table I lists the peak values of the Kirchhoff normal force, the bending moments and corner reactions for a simply-supported square plate under uniformly distributed load. Our values of  $M_x$  and  $M_y$  differ at the centre of the plate because of the asymmetry of the triangular elemental division; this discrepancy is, however, a reflection on the suitability of the chosen size of mesh in relation to the kind of

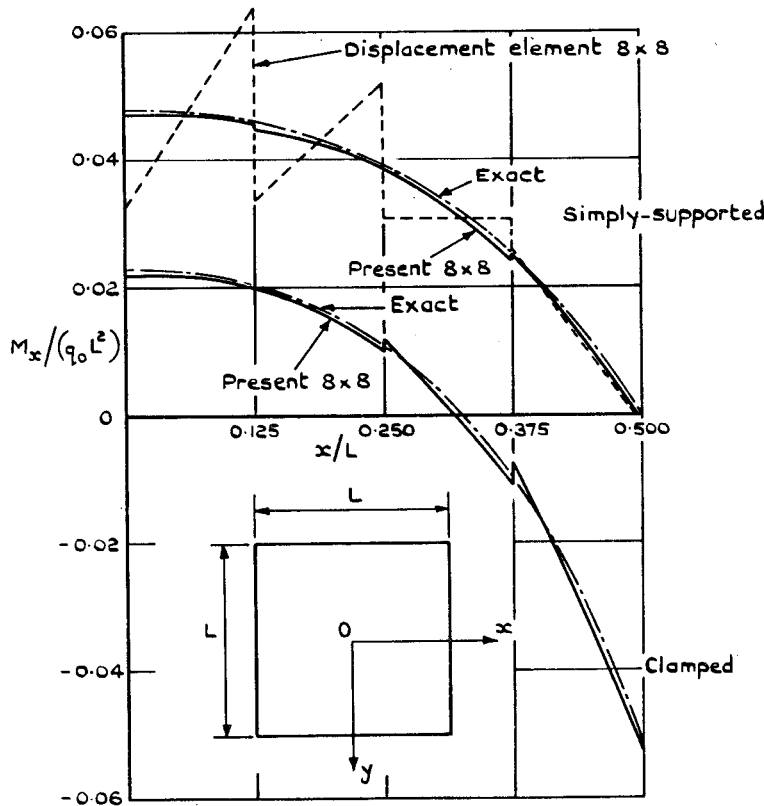


Figure 5. Distribution of  $M_x$  along centre line of square plate under uniformly distributed load.

accuracy required. The exact values and Woinowsky-Krieger<sup>5</sup>. It is seen to within five per cent of these exact Kirchhoff normal force, which involves twisting moments. The last column to the limitation principle of equal overall rate of convergence as the mesh interesting to note that the irregular 4x4 pattern. The quantity  $I(\Omega^2)$  size or pattern; it is numerically equal

$$I(\Omega^2) = \frac{q_0^2}{16(1+\nu)D} \int_{-L/2}^{L/2} \int_{-L/2}^{L/2} (x^2 + y^2) dx dy$$

for a Poisson's ratio  $\nu=0.3$ . Figure 5 shows  $M_x$  along the centre line as calculated very closely to the exact curve. The junctions and it is to be noted that the element is quadratic in virtue of the

CENTRAL DEFLECTION OF A SIMPLY-SUPPORTED SQUARE PLATE UNDER UNIFORM

Mesh	Integration path $w$
2x2	0.00213
4x4A	0.00385
4x4	0.00380
6x6	0.00404
8x8	0.00401
irregular exact	0.00404
	0.00406
Multiplier	$q_0 L^4 / D$

Integration path 1 is taken along a coordinate axis. The arrangement of elements here is not shown which are quoted by Zienkiewicz for comparison.

CLAMPED SQUARE PLATE UNDER UNIFORM

Mesh	Centre of side $M_y$
2x2	-0.0482
4x4A	-0.0395 (-0.0554)
4x4	-0.0544
6x6	-0.0529
8x8	-0.0525
irregular exact	-0.0462 (-0.0581)
	-0.0513
Multiplier	$q_0 L^2$

The alternative values, shown in parentheses, occur when the position coincides with the common vertex of two elements.

accuracy required. The exact values are those quoted in the book by Timoshenko and Woinowsky-Krieger<sup>5</sup>. It is seen that the 8 × 8 mesh provides values which are to within five per cent of these exact values and this remains true even for the Kirchhoff normal force, which involves a higher derivative than the bending and twisting moments. The last column in Table I lists the values calculated according to the limitation principle of equation (44); these provide an indication of the overall rate of convergence as the mesh size decreases and, in this connection, it is interesting to note that the irregular mesh pattern rates only slightly better than the 4 × 4 pattern. The quantity  $I(\Omega^2)$  of equation (45) is independent of the mesh size or pattern; it is numerically equal to

$$I(\Omega^2) = \frac{q_0^2}{16(1+\nu)D} \int_{-L/2}^{L/2} \int_{-L/2}^{L/2} (x^2 + y^2)^2 dx dy = 0.0023371 (8q_0^2 L^6 / D) \quad (54)$$

for a Poisson's ratio  $\nu=0.3$ . Figure 5 shows the distribution of the bending moment  $M_x$  along the centre line as calculated from the 8 × 8 mesh; it is seen to follow very closely to the exact curve. There are only slight discontinuities at the element junctions and it is to be noted that the variation of bending moment within an element is quadratic in virtue of the quadratic variation in  $\Omega(x, y)$  (see equation

**TABLE II**  
CENTRAL DEFLECTION OF A SIMPLY-SUPPORTED SQUARE PLATE UNDER UNIFORMLY DISTRIBUTED LOAD

Mesh	Integration path 1 w	Integration path 2 w	Zienkiewicz <sup>4</sup> w
2 × 2	0.00213	0.00454	0.00220
4 × 4A	0.00385	0.00404	0.00356
4 × 4	0.00380	0.00404	0.00371
6 × 6	0.00404	0.00410	0.00382
8 × 8	0.00401	0.00406	0.00392
irregular	0.00404	0.00408	—
exact	0.00406	0.00406	0.00406
Multiplier	$q_0 L^4 / D$	$q_0 L^4 / D$	$q_0 L^4 / D$

Integration path 1 is taken along a coordinate axis; integration path 2 is taken along a diagonal. The arrangement of elements here is not necessarily identical with that used to obtain the results which are quoted by Zienkiewicz for conforming displacement triangular elements.

**TABLE III**  
CLAMPED SQUARE PLATE UNDER UNIFORMLY DISTRIBUTED LOAD

Mesh	Centre of side $M_y$	Centre of plate $M_x$ $M_y$		Strain energy $-I(\Omega^2)$ is less than (see equation (44))
2 × 2	-0.0482	0.0157	0.0130	-0.00019788
4 × 4A	-0.0395 (-0.0554)	0.0216	0.0189	-0.00020821
4 × 4	-0.0544	0.0216	0.0192	-0.00020794
6 × 6	-0.0529	0.0224	0.0212	-0.00020912
8 × 8	-0.0525	0.0226	0.0220	-0.00020928
irregular	-0.0462 (-0.0581)	0.0228	0.0228	-0.00020900
exact	-0.0513	0.0231	0.0231	—
Multiplier	$q_0 L^2$	$q_0 L^2$	$q_0 L^2$	$8q_0^2 L^6 / D$

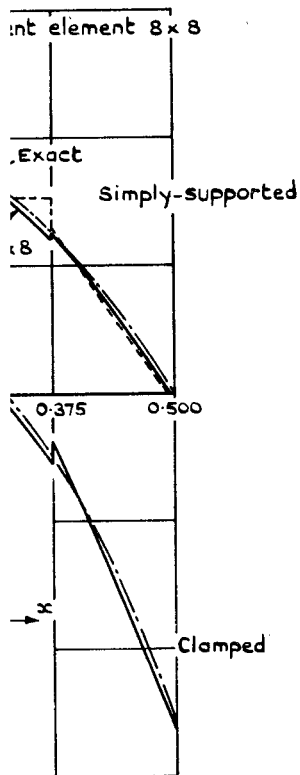
The alternative values, shown in parentheses, occur when the position coincides with the common vertex of two elements.

UNIFORMLY DISTRIBUTED LOAD

Corner reaction $ 2M_{xy} $	Strain energy $-I(\Omega^2)$ is less than (see equation (44))
0.068	-0.00011854
0.069	-0.00012667
0.069	-0.00012658
0.067	-0.00012717
0.067	-0.00012725
0.070	-0.00012701
0.065	—
$q_0 L^2$	$8q_0^2 L^6 / D$

when the position coincides with the

chhoff normal force, the bending  
orted square plate under uniformly  
r at the centre of the plate because  
ision; this discrepancy is, however,  
of mesh in relation to the kind of



quare plate under uniformly distributed

**TABLE IV**  
CENTRAL DEFLECTION OF A CLAMPED SQUARE PLATE UNDER UNIFORMLY DISTRIBUTED LOAD

Mesh	Integration path 1 <i>w</i>	Integration path 2 <i>w</i>	Zienkiewicz <sup>4</sup> <i>w</i>
2x2	-0.00030	0.00107	0.00026
4x4A	0.00096	0.00127	0.00100
4x4	0.00094	0.00129	0.00120
6x6	0.00119	0.00124	0.00116
8x8	0.00121	0.00127	0.00121
irregular exact	0.00123	0.00141	—
exact	0.00126	0.00126	0.00126
Multiplier	$q_0 L^4 / D$	$q_0 L^4 / D$	$q_0 L^4 / D$

Integration path 1 is taken along a coordinate axis; integration path 2 is taken along a diagonal. The arrangement of elements here is not necessarily identical with that used to obtain the results which are quoted by Zienkiewicz for conforming displacement triangular elements.

**TABLE V**  
CLAMPED SQUARE PLATE UNDER CENTRAL CONCENTRATED LOAD

Mesh	Centre of side $M_y$	Centre of plate	
		Integration path 1 <i>w</i>	Integration path 2 <i>w</i>
8x8 exact	-0.1277	0.00560	0.00572 (0.0052)
	-0.1257	0.00560	0.00560
Multiplier	<i>P</i>	$PL^2 / D$	$PL^2 / D$

The value in parentheses is quoted by Zienkiewicz<sup>4</sup> for conforming displacement triangular elements.

**TABLE VI**  
CORNER-SUPPORTED SQUARE PLATE UNDER UNIFORMLY DISTRIBUTED LOAD

Mesh	Centre of side $M_x$	Centre of plate			Strain energy $-I(\Omega^2)$ is less than (see equation (44))
		<i>w</i>	$M_x$	$M_y$	
2x2	0.139 (0.095)	0.0263 (0.0176)	0.090	0.127 (0.095)	0.00092180
4x4A	0.146 (0.149)	0.0258 (0.0232)	0.106	0.115 (0.108)	0.00091817
4x4	0.148 (0.149)	0.0259 (0.0232)	0.106	0.115 (0.108)	0.00091808
6x6	0.149 (0.150)	0.0256 (0.0244)	0.109	0.113 (0.109)	0.00091774
8x8	0.150	0.0256	0.110	0.113	0.00091763
irregular exact	0.148	0.0255	0.111	0.112	0.00091730
exact	0.1527	0.0257	0.1109	0.1109	—
Multiplier	$q_0 L^2$	$q_0 L^4 / D$	$q_0 L^2$	$q_0 L^2$	$8q_0^2 L^6 / D$

The values in parentheses are those of Zienkiewicz<sup>4</sup> for non-conforming displacement rectangular elements. The integration path for calculating *w* is taken along a diagonal.

**TABLE VII**  
DEFLECTIONS OF A SQUARE PLATE WITH CONCENTRIC SQUARE HOLE UNDER UNIFORMLY DISTRIBUTED LOAD

Integration path (see Fig. 8)	Deflection <i>w</i>			
	Point 1		Point 2	
	8x8	12x12	8x8	12x12
AA	0.00218	0.00223	0.00305	0.00311
A'A'	0.00198	0.00207	0.00285	0.00295
BB	0.00196	0.00203	—	—
CC	0.00232	0.00231	—	—
DD	—	—	0.00329	0.00324
Dawe <sup>6</sup>	0.00222	0.00226	0.00314	0.00316
Multiplier	$q_0 L^4 / D$	$q_0 L^4 / D$	$q_0 L^4 / D$	$q_0 L^4 / D$

The values obtained by Dawe are for non-conforming displacement rectangular elements.

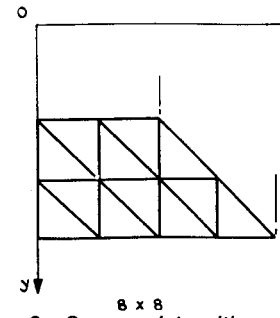
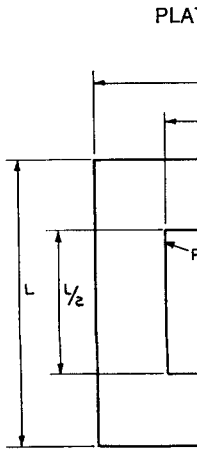


Figure 6. Square plate with com...

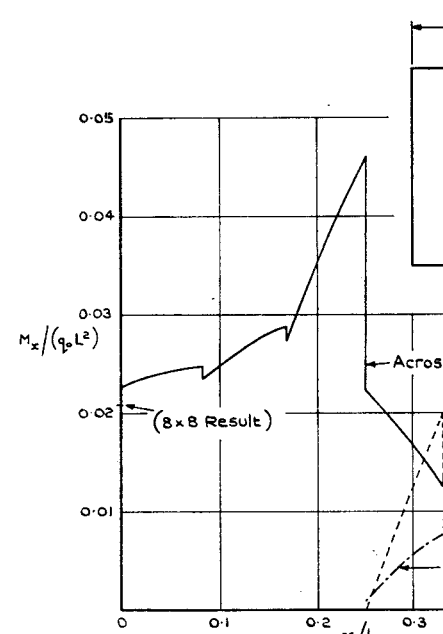


Figure 7. Bending moments in square plate with concentric square hole under uniformly distributed load.

E PLATE UNDER UNIFORMLY

ion path 2 w	Zienkiewicz <sup>4</sup> w
0107	0.00026
0127	0.00100
0129	0.00120
0124	0.00116
0127	0.00121
0141	—
0126	0.00126
$L^4/D$	$q_0 L^4/D$

ion path 2 is taken along a diagonal. al with that used to obtain the results ent triangular elements.

CONCENTRATED LOAD

Centre of plate path 1	Integration path 2 w
50	0.00572 (0.0052)
50	0.00560
$D$	$PL^3/D$

conforming displacement triangular

FORMLY DISTRIBUTED LOAD

$M_y$	Strain energy $-I(\Omega^2)$ is less than (see equation (44))
0.127 (0.095)	0.00092180
0.115 (0.108)	0.00091817
0.115 (0.108)	0.00091808
0.113 (0.109)	0.00091774
0.113	0.00091763
0.112	0.00091730
0.1109	—
$q_0 L^2$	$8q_0^2 L^5/D$

conforming displacement rectangular r ng a diagonal.

CENTRIC SQUARE HOLE UNDER LOAD

Reflection w	Point 2	
	8x8	12x12
3	0.00305	0.00311
7	0.00285	0.00295
3	—	—
1	—	—
5	0.00329	0.00324
5	0.00314	0.00316
	$q_0 L^4/D$	$q_0 L^4/D$

placement rectangular elements.

PLATE BENDING

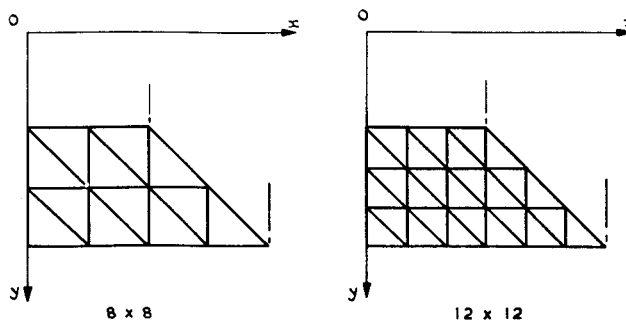
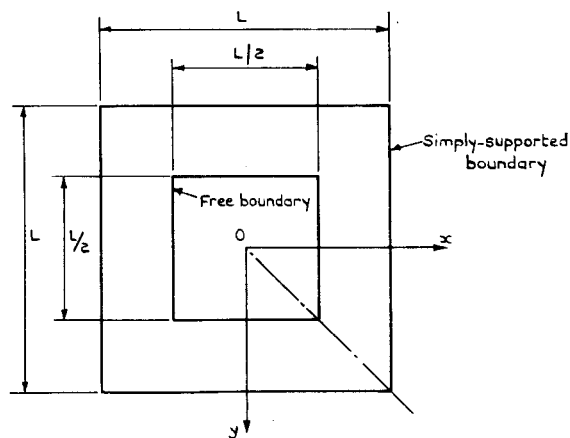


Figure 6. Square plate with concentric square hole. Elemental divisions.

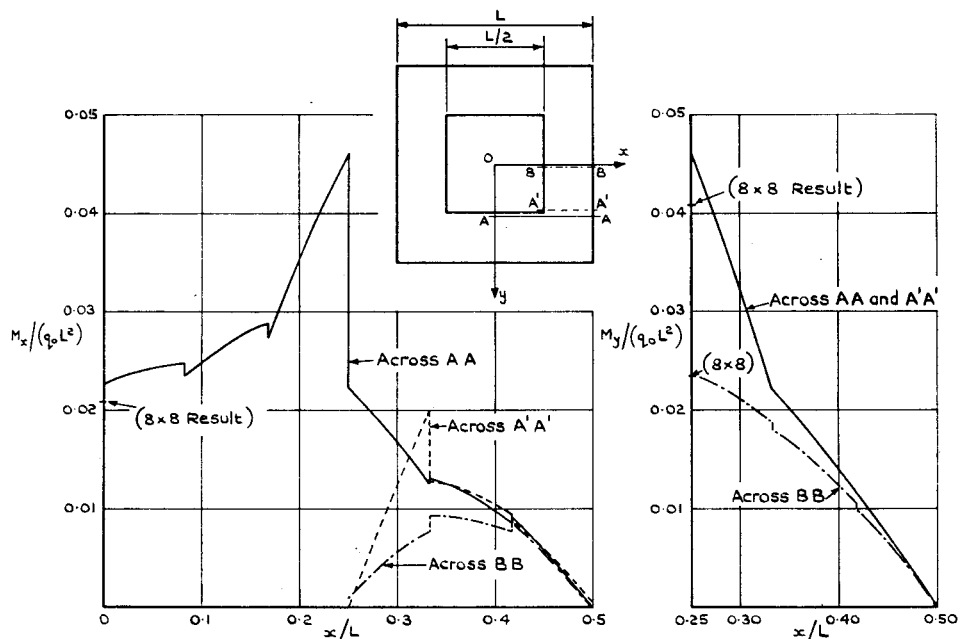


Figure 7. Bending moments in square plate with concentric square hole under uniformly distributed load (12x12).

(52)). The corresponding distribution of  $M_x$  from the non-conforming displacement triangular element displays excessive discontinuities at the element junctions and Zienkiewicz<sup>4</sup> suggests, in practical problems using this element, that attention should be focused at the bending moments at centroids of elements. Values of  $M_x$  for conforming elements are not available. Table II lists values of the central deflection  $w(0,0)$  obtained by the straightforward integration of equation (49) and making use of the fact that  $w=0$  on the boundary and  $\partial w/\partial s=0$  at the centre of the plate. The value calculated for  $w$  is dependent upon the path chosen for integration because, in our equilibrium analysis, we satisfy only approximately the conditions of compatibility. The values listed in the last column of Table II are extracted from Zienkiewicz<sup>4</sup> for conforming displacement triangular elements.

Tables III and IV provide the associated results for the clamped square plate under uniformly distributed load. The distribution of the bending moment  $M_x$  along the centre line, as calculated from the  $8 \times 8$  mesh, is also shown in Fig. 5 and again follows the exact curve very closely. The corresponding distribution from the displacement triangular element is not available. Table V lists comparative values for the case of a central concentrated load using the  $8 \times 8$  mesh.

Zienkiewicz<sup>4</sup> suggests that the finite element analysis of a corner-supported square plate might be expected to cause difficulties because of the concentrations which occur at the corner points. Table VI shows values of the bending moments and deflections along with the comparative results of Zienkiewicz for non-conforming displacement rectangular elements. Reasonable agreement is obtained with the exact values taken from the book by Timoshenko and Woinowsky-Krieger<sup>5</sup> (these values differ slightly from those quoted by Zienkiewicz<sup>4</sup> and attributed to Marcus).

The final problem to be considered here concerns a simply-supported square plate under uniformly distributed load where there is a concentric square hole with free edges, as shown in Fig. 6. It is known that singular behaviour of the bending moments occurs at the internal corner points and its effect upon our finite element

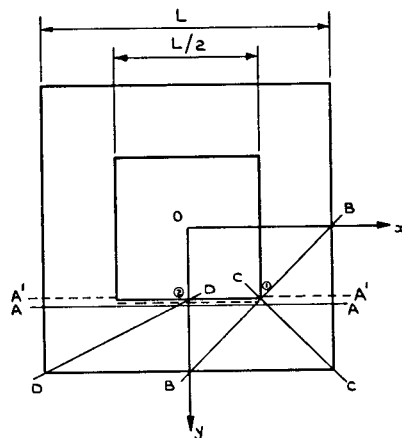


Figure 8. Square plate with concentric square hole. Paths of integration to calculate the deflections.

solution is illustrated by the difference in  $M_x$  through the cross-sections  $AA'$  and  $BB'$ . Figure 7 provides, of course, a finite value even at the corners, but the discontinuities and slow convergence from the singularity. The deflection  $w(0,0)$  is calculated by integrating equation (49) along the paths  $AA'$  and  $BB'$  (Table VII). There is appreciable variation in the sequence of the effects emanating from the singularity, which are given in Table VII are due to the use of the displacement rectangular element instead of the displacement triangular element when applied to this problem provided

strain energy

for the  $8 \times 8$  mesh, and

strain energy

for the  $12 \times 12$  mesh, where the com

### Acknowledgement

This paper is Crown Copyright © 1968, by the Controller, Her Majesty's Stationery Office.

The author is indebted to Mr. J. P. Benthem for his suggestions.

### References

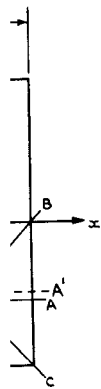
- MORLEY, L. S. D. A triangular finite element method for plate bending problems. *Journal of the Royal Aeronautical Society*, p. 715, October 1967.
- FRAEIJNS DE VEUBEKE, B. Displacement method. In *Stress analysis*, Wiley, New York, 1967.
- ARGYRIS, J. H. Reinforced fields and the effect of initial strain. *Journal of the Royal Aeronautical Society*, p. 100, 1967.
- ZIENKIEWICZ, O. C. *The finite element method*, McGraw-Hill, New York, 1967.
- TIMOSHENKO, S. and WOINOWSKY-KRIEGER, G. *Strength of materials*, McGraw-Hill, New York, 1959.
- DAWE, D. J. On assumed displacement methods. *Journal of the Royal Aeronautical Society*, p. 100, 1967.
- BENTHEM, J. P. Note on minimizing strains by matrix methods, with application to the research institute (Amsterdam) Report No. 10, 1967.

the non-conforming displacement  $w$  at the element junctions and along this element, that attention is paid to the junctions of elements. Values of  $M_x$  in Table II lists values of the central integration of equation (49) and  $\partial w / \partial s = 0$  at the centre of the element. The path chosen for integration is shown in Fig. 7. The values of  $M_x$  in column of Table II are extracted from the analysis of triangular elements.

Results for the clamped square plate are shown in Fig. 5 and the distribution of the bending moment  $M_x$  is also shown in Fig. 5 and the corresponding distribution from Table V lists comparative values using the  $8 \times 8$  mesh.

The analysis of a corner-supported square plate because of the concentrations of values of the bending moments of Zienkiewicz for non-conforming elements. Agreement is obtained with the results of Woinowsky-Krieger<sup>5</sup> (these results are attributed to Marcus).

The analysis concerns a simply-supported square plate with a concentric square hole with angular behaviour of the bending moment and its effect upon our finite element



Paths of integration to calculate

The Aeronautical Quarterly

solution is illustrated by the differences in the distribution of the bending moment  $M_x$  through the cross-sections  $AA$  and  $A'A'$ , as shown in Fig. 7. Our solution provides, of course, a finite value everywhere for  $M_x$  and this leads to appreciable discontinuities and slow convergence in the finite element values for  $M_x$ , even away from the singularity. The deflection  $w$  at the points 1 and 2 (see Fig. 8) is calculated by integrating equation (49) along five different paths and the results are listed in Table VII. There is appreciable variation in the values and this again is a consequence of the effects emanating from the singularity. The comparative values for  $w$  which are given in Table VII are due to Dawe<sup>6</sup>, using a version of his non-conforming displacement rectangular element. The limitation principle of equation (44) when applied to this problem provides

$$\text{strain energy} \leq -0.00017376 + I (\Omega^2)$$

for the  $8 \times 8$  mesh, and

$$\text{strain energy} \leq -0.00017396 + I (\Omega^2)$$

for the  $12 \times 12$  mesh, where the common multiplier is  $8q_0^2 L^6 / D$ .

### Acknowledgement

This paper is Crown Copyright and is reproduced with the permission of the Controller, Her Majesty's Stationery Office.

The author is indebted to Mr. B. C. Merrifield for assistance in the computations.

### References

- MORLEY, L. S. D. A triangular equilibrium element with linearly varying bending moments for plate bending problems. *Journal of the Royal Aeronautical Society*, Vol. 71, p. 715, October 1967.
- FRAEIJNS DE VEUBEKE, B. Displacement and equilibrium models in the finite element method. In *Stress analysis*, Wiley, New York, 1965.
- ARGYRIS, J. H. Reinforced fields of triangular elements with linearly varying strain; effect of initial strain. *Journal of the Royal Aeronautical Society*, Vol. 69, p. 799, 1965.
- ZIENKIEWICZ, O. C. *The finite element method in structural and continuum mechanics*. McGraw-Hill, New York, 1967.
- TIMOSHENKO, S. and WOINOWSKY-KRIEGER, S. *Theory of plates and shells*. McGraw-Hill, New York, 1959.
- DAWE, D. J. On assumed displacements for the rectangular plate bending element. *Journal of the Royal Aeronautical Society*, Vol. 71, p. 722, October 1967.
- BENTHEM, J. P. Note on minimizing a quadratic function with additional linear constraints by matrix methods, with application to stress analysis. National Aeronautical Research Institute (Amsterdam) Report S 437, 1954.



The inverse  $\Gamma_{1c}^{-1}$  is assumed to have a bandwidth denoted here by  $n$ . From equation (A2) we may write

$$q = \Gamma_{1c}^{-1} \gamma_{qc} \tag{A4}$$

and, considering an arbitrary variation of the coefficients  $q$ ,

$$\delta q = \Gamma_{1c}^{-1} \delta \gamma_{qc}, \tag{A5}$$

since  $\delta c_i \equiv 0$ . Now, there is the relationship

$$\gamma_{q0} = \Gamma_{10} q, \tag{A6}$$

so that equation (A5) becomes

$$\delta q = \Gamma_{1c}^{-1} \Gamma_{10} \delta q \tag{A7}$$

and, on substituting into equation (A1), we have

$$\delta q^T \Gamma_{10} \Gamma_{1c}^{-1T} (Kq - g - g') = 0, \tag{A8}$$

where the variations of  $\delta q$  may now be considered as arbitrary.

At this stage, let us note the Theorem which states that *the multiplication of a square matrix of bandwidth  $m$  by another square matrix of bandwidth  $n$  yields a square matrix of bandwidth  $m+n-1$* . Thus, in equation (A8) the square matrix  $\Gamma_{10}$  is of unitary bandwidth,  $\Gamma_{1c}^{-1T}$  has bandwidth  $n$  and, if  $K$  has bandwidth  $m$ , then the product  $\Gamma_{10} \Gamma_{1c}^{-1T} K$  has bandwidth  $m+n-1$ . From the arbitrary variations of equation (A8) we may set up the simultaneous equations

$$\Gamma_{10} \Gamma_{1c}^{-1T} K q = \Gamma_{10} \Gamma_{1c}^{-1T} (g + g'), \tag{A9}$$

where the square matrix  $\Gamma_{10} \Gamma_{1c}^{-1T} K$  is singular because of the rows of zeros awaiting the imposition of the constraint equations (A2). Thus, we finally determine the coefficients  $q_i$  from

$$(\Gamma_{10} \Gamma_{1c}^{-1T} K + \Gamma_{0c}) q = \Gamma_{10} \Gamma_{1c}^{-1T} (g + g') + \gamma_{0c}. \tag{A10}$$

It is particularly worth noting that it is only those element numbers on a boundary where a traction is prescribed which have other than unitary lone diagonal coefficients in  $\Gamma_{1c}$ . For the purpose of obtaining the inverse  $\Gamma_{1c}^{-1}$  it is therefore easy to derive a reduced size matrix which involves only these boundary numbers. Moreover, the product  $\Gamma_{10} \Gamma_{1c}^{-1T}$  can be carried out on the reduced size matrix.

LEY

FUNCTION WITH BANDED LINEAR CONSTRAINTS

is obtained through the variational

$$\delta J = 0, \tag{A1}$$

generally have to suffer linear constraint

$$\tag{A2}$$

way of applying such constraints is more, but this has the disadvantage of being of higher order than  $K$ . There are several methods and one is described by Benthem<sup>7</sup> where every important banded properties. It is noted that these properties can often be preserved without

are of the banded form

$$\begin{bmatrix} q_1 \\ q_2 \\ q_3 \\ q_4 \\ q_5 \\ q_6 \\ q_7 \\ q_8 \\ q_9 \\ q_{10} \\ q_{11} \\ q_{12} \\ q_{13} \\ q_{14} \end{bmatrix} = \begin{bmatrix} q_1 \\ q_2 \\ q_3 \\ q_4 \\ c_5 \\ c_6 \\ q_7 \\ q_8 \\ q_9 \\ q_{10} \\ q_{11} \\ q_{12} \\ c_{13} \\ q_{14} \end{bmatrix} \tag{A3}$$

with a much larger proportion of unitary diagonal notation,  $\Gamma_{0c}$  where all the other elements are placed with zeros,  $\Gamma_{10}$  where the  $C_{ij}$  elements are placed with zeros, where the  $q_i$  coefficients of  $\gamma_{qc}$  are replaced with zeros.